



Published in final edited form as:

Pharmacol Res. 2017 May ; 119: 61–71. doi:10.1016/j.phrs.2017.01.018.

P-gp/ABCBI Exerts Differential Impacts On Brain and Fetal Exposure to Norbuprenorphine

Michael Z. Liao, Chunying Gao, Laura M. Shireman, Brian Phillips, Linda J. Risler, Naveen K. Neradugomma, Prachi Choudhari, Bhagwat Prasad, Danny D. Shen, and Qingcheng Mao*

Department of Pharmaceutics, School of Pharmacy, University of Washington, Seattle, Washington 98195, USA

Abstract

Norbuprenorphine is the major active metabolite of buprenorphine which is commonly used to treat opiate addiction during pregnancy. Norbuprenorphine produces marked respiratory depression and was 10 times more potent than buprenorphine. Therefore, it is important to understand the mechanism that controls fetal exposure to norbuprenorphine, as exposure to this compound may pose a significant risk to the developing fetus. P-gp/ABC1 and BCRP/ABC2 are two major efflux transporters regulating tissue distribution of drugs. Previous studies have shown that norbuprenorphine, but not buprenorphine, is a P-gp substrate. In this study, we systematically examined and compared the roles of P-gp and BCRP in determining maternal brain and fetal distribution of norbuprenorphine using transporter knockout mouse models. We administered 1 mg/kg norbuprenorphine by retro-orbital injection to pregnant FVB wild-type, *Abcb1a^{-/-}/1b^{-/-}* and *Abcb1a^{-/-}/1b^{-/-}/Abcg2^{-/-}* mice on gestation day 15. The fetal AUC of norbuprenorphine was ~64% of the maternal plasma AUC in wild-type mice, suggesting substantial fetal exposure to norbuprenorphine. The maternal plasma AUCs of norbuprenorphine in *Abcb1a^{-/-}/1b^{-/-}* and *Abcb1a^{-/-}/1b^{-/-}/Abcg2^{-/-}* mice were ~2 times greater than that in wild-type mice. Fetal AUCs in *Abcb1a^{-/-}/1b^{-/-}* and *Abcb1a^{-/-}/1b^{-/-}/Abcg2^{-/-}* mice were also increased compared to wild-type mice; however, the fetal-to-maternal plasma AUC ratio remained relatively unchanged by the knockout of *Abcb1a/1b* or *Abcb1a/1b/Abcg2*. In contrast, the maternal brain-to-maternal plasma AUC ratio in *Abcb1a^{-/-}/1b^{-/-}* or *Abcb1a^{-/-}/1b^{-/-}/Abcg2^{-/-}* mice was increased ~30-fold compared to wild-type mice. Protein quantification by LC-MS/MS proteomics revealed significantly higher amounts of P-gp protein in the wild-type mice brain than that in the placenta. These results indicate that fetal exposure to norbuprenorphine is substantial and that P-gp has a minor impact on fetal exposure to norbuprenorphine, but plays a significant role in restricting its brain distribution. The differential impacts of P-gp on norbuprenorphine distribution into the brain and fetus are likely, at least in part, due to the differences in amounts of P-gp protein expressed in

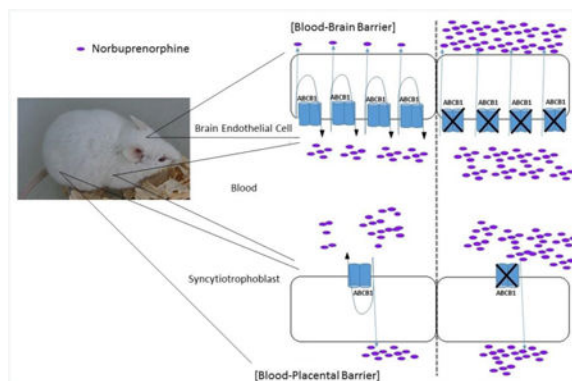
*Corresponding author: Qingcheng Mao, PhD, Department of Pharmaceutics, School of Pharmacy, University of Washington, Box 357610, Seattle, Washington 98195, USA, Phone: +1 206 685 0355, Fax: +1 206 543 3204, qmao@u.washington.edu.

Conflict of interest: All the authors declare no conflict of interest.

Publisher's Disclaimer: This is a PDF file of an unedited manuscript that has been accepted for publication. As a service to our customers we are providing this early version of the manuscript. The manuscript will undergo copyediting, typesetting, and review of the resulting proof before it is published in its final citable form. Please note that during the production process errors may be discovered which could affect the content, and all legal disclaimers that apply to the journal pertain.

the blood-brain and blood-placental barriers. BCRP is not as important as P-gp in determining both the systemic and tissue exposure to norbuprenorphine. Finally, fetal AUCs of the metabolite norbuprenorphine- β -D-glucuronide were 3-7 times greater than maternal plasma AUCs, while the maternal brain AUCs were <50% of maternal plasma AUCs, suggesting that a reversible pool of conjugated metabolite in the fetus may contribute to the high fetal exposure to norbuprenorphine.

Graphical abstract



Keywords

Norbuprenorphine; Pregnancy; ABCB1; ABCG2; Blood-brain barrier; Blood-placental barrier

1. Introduction

Recent statistics indicate that the prevalence of opioid use among pregnant women ranges from 1-2% to as high as 21% in the United States [1], posing a major risk for maternal morbidities and neonatal complications. Methadone and buprenorphine are prescribed to pregnant women to treat opiate addiction [2, 3]. Although the fetus is not the target of treatments, it is exposed to these drugs *de facto* when pregnant women use the medications. Randomized clinical trials comparing methadone and buprenorphine indicate that both medications are effective in preventing relapse to illicit opioids in opioid-dependent patients. Buprenorphine, however, results in less severe neonatal abstinence syndrome than methadone [4].

Buprenorphine (BUP) is a semisynthetic thebaine derivative that acts as a mixed partial agonist- antagonist opioid receptor modulator [5]. BUP undergoes *N*-dealkylation in the liver, forming the major metabolite norbuprenorphine (NBUP). NBUP is pharmacologically active with ~25% of buprenorphine's intrinsic analgesic effect [6]. Furthermore, NBUP is a μ -opioid, δ -opioid, and nociceptin receptor full agonist, and a κ -opioid receptor partial agonist. NBUP produces respiratory depression and was 10 times more potent than buprenorphine in rodents [7, 8] and may be fatal to infants [9]. NBUP can be further glucuronidated at the third carbon to norbuprenorphine-3- β -D-glucuronide (NBUP-G), which is also biologically active [6]. Concheiro et al. [10] showed that both NBUP and NBUP-G could be detected in umbilical cord blood samples 5 hours after administration of

buprenorphine but before delivery with concentrations greater than those of the parent drug, suggesting that the fetus may have been exposed to substantial levels of pharmacologically active metabolites. To better predict fetal exposure and hence fetal safety of NBUP, it is critical that we first understand the mechanisms that control fetal exposure to NBUP and NBUP-G, which are currently still not clear.

P-gp/ABCB1 and BCRP/ABCG2 are the two most important ABC efflux transporters for drug disposition and have a broad spectrum of substrates, including many drugs routinely used by pregnant women [11-13]. P-gp and BCRP are highly expressed on the apical membrane of the liver hepatocyte, the brain endothelium and the placental syncytiotrophoblasts [14-16]. Hence, both transporters restrict penetration across tissue barriers and facilitate biliary elimination of drugs and xenobiotics. For example, it has been shown that P-gp and BCRP can protect the brain and fetus from potential chemical assaults by actively expelling drugs, xenobiotics and harmful substances from the brain or the fetus to the systemic or maternal circulation [17-21].

Previous studies have shown that P-gp can effectively transport NBUP but not BUP [6, 22] and that P-gp is a major determinant of brain NBUP exposure [6]. BCRP is known to transport glucuronide conjugates of drugs, xenobiotics, and endogenous substances [23]. Given the fact NBUP is a P-gp substrate and NBUP-G is possibly a BCRP substrate, it is important to know whether P-gp or BCRP restricts fetal exposure to NBUP and/or its glucuronide metabolite. Murine knockout models have been developed to interrogate the effects of P-gp and BCRP on drug disposition [24-27]. Numerous studies using chemical inhibition and genetic knockout of P-gp and BCRP have demonstrated the importance of the two transporters in determining brain or fetal distribution of several prototypic substrates, including methadone, loperamide, fentanyl, glyburide, and nitrofurantoin [18, 19, 28-33]. Therefore, the aim of this study was to investigate whether P-gp and BCRP affect maternal pharmacokinetics of NBUP and its metabolite NBUP-G and whether P-gp and BCRP play important roles in restricting fetal penetration of NBUP and NBUP-G, using wild-type, *Abcb1a^{-/-}/1b^{-/-}*, and *Abcb1a^{-/-}/1b^{-/-}/Abcg2^{-/-}* pregnant mice. It has previously been shown that P-gp in the blood-brain barrier (BBB) and the blood-retinal barrier (BRB) of mouse models has dissimilar impacts on tissue exposure to a substrate drug verapamil, with a much greater effect on limiting brain exposure than retinal exposure [34]. Hence, to investigate whether P-gp and BCRP in the BBB and the blood-placental barrier (BPB) display differential roles in restricting brain and fetal drug exposure, we also examined and compared brain and fetal exposure to NBUP and NBUP-G in the same wild-type and transporter knockout dams.

2. Methods and methods

2.1. Materials

Norbuprenorphine (NBUP) and norbuprenorphine-3- β -D-glucuronide (NBUP-G) used in animal studies were provided by the National Institute on Drug Abuse (Bethesda, MD). NBUP, norbuprenorphine-d3 (NBUP- d3) and NBUP-G used for analytical calibrations in LC-MS/MS analysis were from Cerilliant (Round Rock, TX). Optima grade or high-performance liquid chromatography grade methanol, acetonitrile, polyethylene glycol 400,

ethanol, formic acid, DMSO, dimethyl sulfoxide and water were from Thermo Fisher Scientific (Waltham, MA) or Acros Organics (Pittsburgh, PA). Isoflurane was purchased from Piramal Healthcare (Mumbai, India) through the University of Washington Medical Center Pharmacy. Synthetic signature peptides for absolute protein quantification by LC-MS/MS were obtained from New England Peptides (Boston, MA). The corresponding stable-isotope-labeled (SIL) peptides were purchased from Thermo Fisher Scientific (Rockford, IL). The protein extraction kit for ProteoExtract native membrane was from Calbiochem (Temecula, CA). Ammonium bicarbonate and sodium deoxycholate were obtained from Thermo Fisher Scientific and MP Biomedicals (Santa Ana, CA), respectively. BCA protein assay and in-solution trypsin digestion kits, iodoacetamide and dithiothreitol were obtained from Pierce Biotechnology (Rockford, IL).

2.2. Animals

Wild-type FVB, *Abcb1a^{-/-}/1b^{-/-}*, and *Abcb1a^{-/-}/1b^{-/-}* mice, 7-10 weeks of age, were purchased from Taconic Farms (Germantown, NY) and cared for in accordance with the Guide for the Care and Use of Laboratory Animals published by the National Research Council. Mice were maintained under 12-hour light/dark cycles, and food was provided ad libitum. Female mice, 7-10 weeks of age, were mated with male mice of the same genotype and the same age overnight using a female to male ratio of 2:1. Gestation day (gd) 1 was defined as the presence of a sperm plug following overnight housing. Progress of pregnancy was monitored by visual inspection and body weight increase. Body weight was recorded on the day of dosing. Pregnant mice used in this study were on gd 15, which approximately corresponds to the late second trimester in humans. On gd 15, high levels of both P-gp and BCRP are expressed in mouse placenta, and hence gd 15 was chosen in this study [35-37]. This animal protocol was approved by the Institutional Animal Care and Use Committee of the University of Washington.

2.3. In vivo animal studies

NBUP was dissolved in a solution that contained 0.5 % (v/v) dimethyl sulfoxide, 10% (v/v) ethanol, 39.5% (v/v) saline, and 50% (v/v) polyethylene glycol 400 at a concentration of 0.5 mg/ml. Under 2-5% isoflurane anesthesia, pregnant mice on gd 15 were administered 1 mg/kg NBUP by retro-orbital injection (6070 μ l each mouse). The 1 mg/kg dose was selected based on literature data about elicitation of a significant decrease in respiratory rate in mice and achievement of maternal plasma exposure of NBUP in mice that was comparable to that observed in pregnant women in the late second and early third trimesters [6, 38, 39]. Previous pharmacokinetic studies indicated that the half-life of NBUP in rodents was approximately 0.9 hour [40]. We therefore administered NBUP to pregnant mice and collected blood at time points up to 480 min which is longer than 7 half-lives. Thus, at various times (2, 10, 30, 120, 240, 360, and 480 min) after NBUP administration, mice (n = 3 per time point) were sacrificed under anesthesia by cardiac puncture. Maternal blood was collected in heparinized microcentrifuge tubes (BD Bioscience, San Jose, CA) and centrifuged at 1,000 RCF for 10 min at 4°C. Plasma was collected and stored at -80°C until use. Maternal liver and brain as well as individual whole fetuses and placentas were collected from pregnant mice immediately following collection of maternal blood. All the

tissues were immediately rinsed with ice-cold PBS, snap-frozen in liquid nitrogen, and stored at -80°C until analysis.

2.4 Simultaneous quantification of NBUP and NBUP-G in maternal plasma and tissues by LC-MS/MS

Maternal brain, maternal liver and fetus were homogenized in 1.0 ml of PBS using an Omni Bead Ruptor Homogenizer (Omni International, Kennesaw, GA) (see below). To every 500 µl of maternal plasma, brain/fetus homogenate or maternal liver extract, 1 ml of acetonitrile and 20 µl of internal standard (2 ng/µl NBUP-d3) were added and mixed. Samples were vortexed for 30 s and centrifuged at 24,000 rpm for 10 min at 4°C. Supernatants were transferred to clean glass tubes and evaporated using nitrogen gas. Maternal liver homogenate was subjected to solid-phase extraction (SPE) with preconditioned Agilent Bond Elut C₈ cartridges (Santa Clara, CA). Each sample was reconstituted with 100 µl of 1% formic acid in acetonitrile and 5 µl per sample were injected for LC-MS/MS analysis. Calibration curves and quality control samples were prepared along with samples by homogenizing blank tissues and adding analytical grade NBUP or NBUP-G at various concentrations.

Quantification of NBUP and NBUP-G in maternal plasma as well as maternal brain, maternal liver and fetal homogenates by LC-MS/MS was as previously described with some modifications [41]. Briefly, quantification of NBUP and NBUP-G was performed on Agilent 1290 ultra-high-performance liquid chromatograph interfaced with an Agilent 6410B triple-quadrupole mass spectrometer (Agilent Technologies, Palo Alto, CA). The mass spectrometer was operated in positive ion electrospray ionization mode. Chromatographic separation was performed on an Agilent Poroshell 120 SB-C18 column (2.1 mm × 55 mm, 2.7 µm) (Santa Clara, CA). The injection volume was 5 µl and the column oven temperature was 35°C. The HPLC mobile phase (operated at the rate of 0.4 ml/min) was (A) 0.1% formic acid and (B) methanol. The gradient was maintained at 30% B from 0 to 4 min, increased to 35% B from 4 to 6 min, then declined to 30% B from 6 to 6.5 min, and equilibrated at 30% B until 8 min. Under these conditions, retention times of NBUP and NBUP-G were 6.54 min and 1.91 min, respectively. Both Q1 and Q3 quadrupoles and mass spectrometer conditions were optimized for each analyte. The ionization and fragmentation parameters were set as follows: capillary voltage, 2800 V; gas temperature, 350°C; gas flow rate, 10 L/min; nebulizer, 35 psi; fragmentor, 235 V for NBUP-G and 195 V for NBUP; collision energy, 36 V for NBUP-G and 60 V for NBUP. Multiple reaction monitoring transitions for each analyte and internal standard were m/z 414.2>83.1 for NBUP, m/z 590.3>414.2 for NBUP-G, and m/z 417.2>83.1 for NBUP-d3. NBUP-d3 was used as an internal standard for both NBUP and NBUP-G. NBUP and NBUP-G in maternal plasma and tissues were quantified using peak area ratios (NBUP or NBUP-G to NBUP-d3) with calibration curves and quality controls prepared using analytical grade NBUP or NBUP-G dispensed in matching blank mouse matrix (plasma or tissues). The lower quantification limits were 0.5 ng/ml and 2.5 ng/ml for NBUP and NBUP-G, respectively, in maternal plasma. The lower quantification limits were 1 ng/g and 5 ng/g for NBUP and NBUP-G, respectively, in all tissues. For NBUP quantification in both plasmas and tissues, intraday

and interday variations were 3.7% and 3.8%, respectively. Intraday and interday variations were 2.7% and 5%, respectively, for NBUP-G quantification in plasma and tissues.

2.5. Absolute protein quantification of Abcb1a and Abcb1b in maternal brain and placenta by LC-MS/MS

Absolute protein quantification of Abcb1a and Abcb1b was carried out using a surrogate peptide-based LC-MS/MS method as previously described [42]. Two signature peptides unique for Abcb1a and Abcb1b (Table 1) that are not present in any other known proteins were selected for quantification of each transporter based on previously reported criteria [42]. The selected signature peptide sequences were NTTGALTTR and NSTGSLTTR for murine Abcb1a and Abcb1b, respectively. The corresponding heavy peptides containing labeled [$^{13}\text{C}_6$ $^{15}\text{N}_2$]-lysine or [$^{13}\text{C}_6$ $^{15}\text{N}_4$]-arginine were used as internal standards. Prior to protein quantification, maternal brain and placenta tissues were homogenized in extraction buffer I of the ProteoExtract native membrane protein extraction kit (Calbiochem, Temecula, CA) containing protease inhibitor cocktail according to the manufacturer's instruction. The resulting homogenate was centrifuged at 16,000 RCF for 15 min and the supernatant was discarded. The pellet was resuspended in 1 ml of extraction buffer II with protease inhibitor cocktail and incubated with gentle shaking for 30 min at 4°C followed by centrifugation at 16,000 RCF for 15 min at 4°C. The concentration of total isolated membrane proteins in the supernatant was then determined using the BCA protein assay. The supernatant was diluted to protein concentration of 2 µg per µl or lower. Isolated total membrane proteins were reduced, denatured, alkylated and digested as per our previously reported protocol [43]. Samples were stored at -80°C until analysis.

Abcb1a and Abcb1b were quantified using optimized parameters (Table 1) using AB Sciex Triple Quad 6500 system (Framingham, MA) coupled to Waters® Acquity™ UPLC system (Waters, Hertfordshire, UK). A UPLC column (Acquity UPLC® HSS T3 1.8 µm, 2.1 × 100 mm, Waters) with a Security Guard column (C₁₈, 4 mm × 2.0 mm) from Phenomenex (Torrance, CA) was eluted (0.3 mL/min) with a gradient mobile phase consisting of water and acetonitrile (with 0.1 formic acid; see below). The injection volume was 5 µL (~10 µg of total protein). The mobile phase gradient conditions were 97% A (water containing 0.1% v/v formic acid) and 3% B (acetonitrile containing 0.1% v/v formic acid) held for 3 min, followed by four steps of linear gradient of mobile phase B concentration of 3% to 13%, 13% to 25%, 25% to 50% and 50% to 80% over 3-10 min, 10-20 min, 20-24 min and 24.1-25 min, respectively. This was followed by a washing step using 80% mobile phase B for 0.9 min, and re-equilibration for 4.9 min. The parent to product ion transitions for the analyte peptides and their respective SIL peptides were monitored using optimized LC-MS/MS parameters (Table 1) in ESI positive ionization mode.

2.6. Pharmacokinetic data analysis

Maternal plasma, maternal brain, maternal liver, and fetal area-under-the-curve (AUC) concentration values over 0 to 480 min were calculated using the trapezoidal method for each combination of genotype, analyte, and tissue. Adopting a method similar to one described previously [44], 95% confidence intervals of the AUC sample distributions were estimated by bootstrapping the concentration-time data for each genotype- analyte-tissue

group. Concentration-time points from the genotype-analyte-tissue dataset of interest were randomly sampled with replacement, the AUC was calculated, and the process was repeated for 10,000 iterations. The 95% confidence interval was the range of AUCs that encompassed the 2.5th to the 97.5th percentiles of the sample distribution. Confidence intervals of AUC ratios were also estimated by bootstrapping 10,000 iterations of the paired tissue to plasma AUCs and metabolite to parent AUCs. For comparisons between genotypes, the null distribution was estimated by the following bootstrapping procedure. Concentration-time points from the two genotypes under comparison were combined, randomly sampled with replacement, and assigned to either genotype with 10,000 iterations. The mixed data generated were used to calculate the AUC and AUC ratios for each genotype, and the distribution of the bootstrapped data was considered an estimate of the null distribution. The *p* value for the comparison between genotypes was calculated as the percent of the iterations that the actual sampled data resulted in a more extreme AUC and AUC ratios comparison than the bootstrapped estimate of the null distribution. Values were corrected for multiple testing using the Bonferroni correction. The differences were considered statistically significant if the *p* values were less than 0.05.

3. Results

3.1. The knockout of *Abcb1a/1b* increases systemic exposure to NBUP and NBUP-G

To assess the roles of P-gp and BCRP in determining maternal plasma exposure to NBUP and NBUP-G, NBUP was administered to wild-type, *Abcb1a^{-/-}/1b^{-/-}* and *Abcb1a^{-/-}/1b^{-/-}/Abcg2^{-/-}* pregnant mice on gd 15 by retro-orbital injection of 1 mg/kg NBUP. Fig. 1 depicts mean maternal plasma concentration-time profiles of NBUP (Fig. 1a) and NBUP-G (Fig. 1b) over 480 min. Table 2 presents the maternal plasma AUC_{0-480min} data on NBUP and NBUP-G. Mean maternal plasma concentrations of NBUP and NBUP-G in *Abcb1a^{-/-}/1b^{-/-}* and *Abcb1a^{-/-}/1b^{-/-}/Abcg2^{-/-}* mice showed similar increases at times up to 240 min compared to those in wild-type mice (Fig. 1). At 360 and 480 min, maternal plasma concentrations of NBUP, but not NBUP-G, were higher in *Abcb1a^{-/-}/1b^{-/-}* and *Abcb1a^{-/-}/1b^{-/-}/Abcg2^{-/-}* mice compared to those in wild-type mice (Fig. 1). Consequently, maternal plasma AUC_{0-480min} of NBUP in *Abcb1a^{-/-}/1b^{-/-}* and *Abcb1a^{-/-}/1b^{-/-}/Abcg2^{-/-}* mice was significantly higher by 1.8- and 2.2-fold, respectively, compared to that in wild-type mice (Table 2). Maternal plasma AUC_{0-480min} of NBUP-G in *Abcb1a^{-/-}/1b^{-/-}* and *Abcb1a^{-/-}/1b^{-/-}/Abcg2^{-/-}* mice was also significantly higher by 3.6- and 4.4-fold, respectively (Table 2). No significant differences in maternal plasma AUCs of NBUP and NBUP-G between *Abcb1a^{-/-}/1b^{-/-}* and *Abcb1a^{-/-}/1b^{-/-}/Abcg2^{-/-}* mice were observed.

In wild-type mice, maternal plasma concentrations of NBUP-G were approximately 4-9 times higher than those of NBUP at each time point over 480 min (Fig. 1), leading to a maternal plasma NBUP-G/NBUP AUC ratio of 4.6 (Table 2). The knockout of *Abcb1a/1b* or *Abcb1a/1b/Abcg2* increased maternal plasma NBUP-G/NBUP AUC ratio ~2-fold compared to wild-type mice (Table 2). This increase in maternal plasma AUC of the metabolite NBUP-G in *Abcb1a^{-/-}/1b^{-/-}* and *Abcb1a^{-/-}/1b^{-/-}/Abcg2^{-/-}* mice could be due to an increase in hepatic availability of the parent NBUP for access to metabolism in the liver. Thus, we determined concentrations of NBUP in maternal livers over 480 min as shown in Fig. 2 and calculated

the maternal liver AUC0-480min. As expected, the maternal liver AUC0-480min of NBUP in *Abcb1a^{-/-}/1b^{-/-}* or *Abcb1a^{-/-}/1b^{-/-}/Abcg2^{-/-}* mice was significantly higher by ~2-fold compared to that in wild-type mice (Table 3). Maternal liver AUC0-480min of NBUP-G in *Abcb1a^{-/-}/1b^{-/-}* or *Abcb1a^{-/-}/1b^{-/-}/Abcg2^{-/-}* mice also significantly increased by ~2 fold (Table 3). There were no significant differences in maternal liver AUCs of NBUP and NBUP-G between *Abcb1a^{-/-}/1b^{-/-}* and *Abcb1a^{-/-}/1b^{-/-}/Abcg2^{-/-}* mice.

3.2. Maternal brain exposure to NBUP is strongly limited by *Abcb1a/1b*, but not by *Abcg2*

We next examined maternal brain exposure to NBUP in wild-type, *Abcb1a^{-/-}/1b^{-/-}* and *Abcb1a^{-/-}/1b^{-/-}/Abcg2^{-/-}* mice. As shown in Fig. 3a, maternal brain concentrations of NBUP in *Abcb1a^{-/-}/1b^{-/-}* or *Abcb1a^{-/-}/1b^{-/-}/Abcg2^{-/-}* mice were approximately 10-100 times higher than those in wild-type mice at all times over 480 min. The maternal brain AUC0-480min of NBUP in *Abcb1a^{-/-}/1b^{-/-}* or *Abcb1a^{-/-}/1b^{-/-}/Abcg2^{-/-}* mice was significantly increased 54-60-fold compared to that in wild-type mice, respectively (Table 4). No significant difference in maternal brain AUC between *Abcb1a^{-/-}/1b^{-/-}* and *Abcb1a^{-/-}/1b^{-/-}/Abcg2^{-/-}* mice was observed. Likewise, the maternal brain-to-maternal plasma AUC ratio of NBUP in *Abcb1a^{-/-}/1b^{-/-}* or *Abcb1a^{-/-}/1b^{-/-}/Abcg2^{-/-}* mice was significantly increased 25 to 34-fold compared to that in wild-type mice (Table 4). Again, the maternal brain-to-maternal plasma AUC ratio for NBUP was not significantly different between *Abcb1a^{-/-}/1b^{-/-}* and *Abcb1a^{-/-}/1b^{-/-}/Abcg2^{-/-}* mice, suggesting that the knockout of *Abcg2* had no additional effect on maternal brain exposure to NBUP.

We also compared maternal brain exposure to NBUP-G in wild-type, *Abcb1a^{-/-}/1b^{-/-}* and *Abcb1a^{-/-}/1b^{-/-}/Abcg2^{-/-}* mice. The maternal brain concentrations of NBUP-G in *Abcb1a^{-/-}/1b^{-/-}* and *Abcb1a^{-/-}/1b^{-/-}/Abcg2^{-/-}* mice were 2-5 times higher than those in wild-type mice (Fig. 3b). Maternal brain concentrations of NBUP-G in *Abcb1a^{-/-}/1b^{-/-}/Abcg2^{-/-}* mice were consistently higher than those in *Abcb1a^{-/-}/1b^{-/-}* mice at most time points over 480 min (Fig. 3b). Consequently, maternal brain AUC0-480min of NBUP-G in *Abcb1a^{-/-}/1b^{-/-}* and *Abcb1a^{-/-}/1b^{-/-}/Abcg2^{-/-}* mice was higher by 2.2- and 5.2-fold, respectively, as compared to that in wild-type mice (Table 4), *Abcb1a^{-/-}/1b^{-/-}/Abcg2^{-/-}* mice brain exposure was significantly higher than wild-type mice. However, the maternal brain-to-maternal plasma AUC ratio for NBUP-G was not significantly changed by the knockout of *Abcb1a/1b* or *Abcb1a/1b/Abcg2*, with the fold-change varying from 0.62 to 1.3.

3.3. *Abcb1a/1b* and *Abcg2* do not restrict fetal distribution of NBUP and NBUP-G

Finally, we investigated whether the knockout of *Abcb1a/1b* and *Abcb1a/1b/Abcg2* had any effects on fetal exposure to NBUP and NBUP-G as they did on maternal brain exposure. As shown in Fig. 4, fetal concentrations of NBUP in *Abcb1a^{-/-}/1b^{-/-}* and *Abcb1a^{-/-}/1b^{-/-}/Abcg2^{-/-}* mice were generally higher than those in wild-type mice (Fig. 4a). As a result, fetal AUC0-480min of NBUP in *Abcb1a^{-/-}/1b^{-/-}* and *Abcb1a^{-/-}/1b^{-/-}/Abcg2^{-/-}* mice was significantly increased 1.6-fold as compared to that in wild-type mice (Table 5). The fetal-to-maternal plasma AUC ratio of NBUP remained relatively unchanged in wild-type, *Abcb1a^{-/-}/1b^{-/-}* and *Abcb1a^{-/-}/1b^{-/-}/Abcg2^{-/-}* mice, with AUC ratios of 0.5-0.6. These results indicate that the increase in fetal NBUP exposure in transporter knockout mice is most likely

driven indirectly by the increase in maternal plasma exposure, and not directly by the knockout of placental *Abcb1a/1b* or *Abcb1a/1b/Abcg2*.

Fetal concentrations of NBUP-G in *Abcb1a^{-/-}/1b^{-/-}* and *Abcb1a^{-/-}/1b^{-/-}/Abcg2^{-/-}* mice were significantly higher than those in wild-type mice at 6 h and 8 h (Fig. 4b). Fetal AUC_{0-480min} of NBUP-G in *Abcb1a^{-/-}/1b^{-/-}* and *Abcb1a^{-/-}/1b^{-/-}/Abcg2^{-/-}* mice was significantly higher by 1.7- and 2.0-fold, respectively, as compared to that in wild-type mice (Table 5). The fetal-to-maternal plasma AUC ratios of NBUP-G in *Abcb1a^{-/-}/1b^{-/-}* and *Abcb1a^{-/-}/1b^{-/-}/Abcg2^{-/-}* mice were decreased by ~45% compared to that in wild-type mice. This decrease was due to much greater maternal NBUP-G exposure in *Abcb1a^{-/-}/1b^{-/-}* and *Abcb1a^{-/-}/1b^{-/-}/Abcg2^{-/-}* mice versus wild-type mice. No significant differences in fetal NBUP-G exposure between *Abcb1a^{-/-}/1b^{-/-}* and *Abcb1a^{-/-}/1b^{-/-}/Abcg2^{-/-}* mice were observed (Table 5). Notably, no matter whether in wild-type or transporter knockout mice, fetal AUCs of NBUP-G were 54-65 times higher than fetal AUCs of NBUP (Table 5).

3.4. P-gp protein levels in maternal brain and placenta were quantitatively determined by targeted proteomics

One possible explanation of the dissimilar impacts of P-gp on maternal brain and fetal exposure to NBUP could be differential P-gp protein expression in the brain and placenta. We therefore quantified absolute amounts of P-gp protein (both *Abcb1a* and *Abcb1b*) in maternal mouse brain and placenta tissues by LC-MS/MS proteomic analysis. The protein levels of *Abcb1a* and *Abcb1b* per μg of total membranes in whole mouse placenta were comparable to those in whole maternal mouse brain (Fig. 5a). Since only trophoblasts or brain microvessels are the cells that form the BPB and BBB, respectively, we would have to consider the amounts of *Abcb1a* and *Abcb1b* in cells that form the tissue barriers, rather than the amounts of the transporters in whole tissues. Given the percentage of trophoblasts and brain microvessels out of total numbers of cells in the mouse placenta and brain (~50% [45] and ~6% [46], respectively, on gd 15), the abundance of *Abcb1a* and *Abcb1b* protein in cells that form the blood-tissue barriers in each tissue was calculated to represent an estimate of the overall P-gp density and expressed as fmol of *Abcb1a* and/or *Abcb1b* protein in trophoblasts or brain microvessel endothelial cells that form the BPB or the BBB, respectively, per g of tissue as follows: [P-gp concentration in total membrane proteins (fmol/ μg membrane protein) \times yield of membrane protein isolation ($\mu\text{g}/\text{g}$ tissue)] divided by the percentage of trophoblasts out of total cells in the placenta (50%) or the percentage of brain microvessel endothelial cells out of total cells in maternal brain (6%). The yield of total membrane protein isolation from the placenta or maternal brain varied between 60 – 100 $\mu\text{g}/\text{g}$ tissues. Thus, the relative abundance (or density) of *Abcb1a* and *Abcb1b* protein in the BBB was ~8.4 and ~3.9 times greater than that in the BPB, respectively (Fig. 5b). The relative abundance (or density) of the sum of *Abcb1a/1b* protein in the BBB was ~6.3 times greater than that in the BPB (Fig. 5b). The main assumptions we used in this estimation are that 1) the number of cells is proportional to the weight of cells; 2) all the trophoblasts in the labyrinth zone of mouse placenta are the cells that form the BPB; 3) P-gp is only expressed in brain endothelial cells or placental trophoblasts that form tissue barriers. Indeed, previous studies have shown that P-gp is highly concentrated in endothelial cells of the brain [47] and syncytiotrophoblasts of the placenta [48].

Discussion

BUP is increasingly used as an alternative to methadone for treatment of opiate addiction in the pregnant population, as BUP exposure has been associated with lower neonatal abstinence syndrome scores [49, 50]. However, BUP exhibits a ceiling respiratory effect and its primary active metabolites NBUP and NBUP-G are the potent respiratory depressors in young children. Fetal exposure to NBUP and NBUP-G therefore poses significant risks to the developing fetus. To predict fetal exposure and fetal safety of NBUP, it is important that we first understand the mechanisms that control fetal exposure to NBUP and NBUP-G. In this study, we characterized the roles of P-gp/ABCB1 and BCRP/ABCG2 in modulating penetration of NBUP and NBUP-G across the BBB and BPB using transporter knockout mouse models. At present, little is known regarding the impacts of ABC efflux transporters on fetal exposure to opioids.

We found that, after retro-orbital injection which mimics intravenous administration, maternal plasma AUC of NBUP was significantly increased about 2-fold by the knockout of *Abcb1a/1b*, but additional knockout of *Abcg2* had no further effect (Fig. 1a and Table 2). This suggests that P-gp likely facilitates biliary excretion of NBUP, which is consistent with the fact that NBUP is a substrate of P-gp, but not BCRP [22]. Maternal plasma AUC of NBUP-G was also concurrently increased 3-4-fold and the NBUP-G/NBUP maternal plasma AUC ratio was increased ~2-fold, by the knockout of *Abcb1a/1b* (Table 2). In contrast, additional knockout of *Abcg2* had no significant further effect on systemic NBUP-G exposure (Table 2). This increase in NBUP-G/NBUP maternal plasma AUC ratio may be explained by one or more of the following factors: 1) a decrease in metabolite clearance; 2) an increase in metabolite formation; and 3) an increase in hepatic bioavailability of NBUP for access to metabolism in the liver. To the best of our knowledge, no data is currently available regarding the effects of the knockout of *Abcb1a/1b* on expression of metabolizing enzymes or transporters for NBUP disposition that may result in the first two scenarios. The third scenario would be expected due to lack of canalicular P-gp in *Abcb1a^{-/-}/1b^{-/-}* mice to efflux norbuprenorphine into the bile. The inefficiency of norbuprenorphine biliary elimination may result in the apparent increase in hepatic bioavailability. To test this possibility, we analyzed concentrations and exposure of NBUP in maternal mouse livers and noted that maternal liver AUC of NBUP were indeed significantly increased 2.3-fold by the knockout of *Abcb1a/1b* (Table 3), suggesting that the increase in systemic exposure to NBUP-G is likely caused by the increase in amounts of NBUP available for metabolism in the liver. Nevertheless, the possibility that the knockout of *Abcb1a/1b* alters expression of metabolizing enzymes and transporters and ultimately affects NBUP disposition cannot be completely ruled out.

The site of action of NBUP as an opioid receptor agonist is in the brain. Previous studies have shown that P-gp is a major determinant of brain exposure to NBUP [6]. We noted that maternal brain AUC of NBUP was increased 60-fold by the knockout of *Abcb1a/1b*, but additional knockout of *Abcg2* had no further effect (Fig. 3a and Table 4). Likewise, the maternal brain-to-maternal plasma AUC ratio of NBUP was increased 34-fold by the knockout of *Abcb1a/1b* and additional knockout of *Abcg2* did not further increase the AUC ratio (Table 4). These results again support the notion that P-gp plays a pivotal role in

restricting maternal brain NBUP exposure, which is consistent with previous studies [6]. We found that maternal brain AUC of NBUP-G was increased ~2-fold by the knockout of *Abcb1a/1b*, but its maternal brain-to-maternal plasma AUC ratio was decreased by 25% (Table 4), suggesting that P-gp is not a determining factor for brain NBUP-G exposure. Additional knockout of *Abcg2* further increased maternal brain AUC of NBUP-G more than ~2-fold over maternal brain NBUP-G exposure in *Abcb1a^{-/-}/1b^{-/-}* mice (Table 4), indicating that brain penetration of NBUP-G is restricted by *Abcg2*. This is consistent with the notion that NBUP-G is possibly a BCRP, but not P-gp substrate, based upon current understanding of substrate specificity for P-gp and BCRP.

We determined that fetal AUC of NBUP was ~64% of maternal plasma AUC in wild-type mice (Fig. 4 and Table 5); in contrast, maternal brain AUC of NBUP accounted for ~20% of maternal plasma AUC (Table 4), suggesting that fetal NBUP exposure is substantial. Caution therefore should be taken regarding fetal safety of NBUP when BUP is used by pregnant women given the fact that maternal plasma concentrations of NBUP could be as high as or even greater than those of BUP in pregnant women [51]. We also found that fetal AUC of NBUP was increased 1.6 fold by the knockout of *Abcb1a/1b* or *Abcb1a/1b/Abcg2*, but its fetal-to-maternal plasma AUC ratio remained relatively unchanged (Table 5), indicating that the increase in fetal NBUP exposure in *Abcb1a^{-/-}/1b^{-/-}* and *Abcb1a^{-/-}/1b^{-/-}/Abcg2^{-/-}* mice is primarily driven by the increase in maternal plasma exposure. Therefore, unlike in the BBB, P-gp in the BPB plays a minor role in restricting fetal NBUP exposure. Recently, Eyal et al. showed that chemical inhibition of P-gp in non-human primate increased maternal brain distribution of [¹¹C]-verapamil ~4-fold, but its fetal liver distribution (as a surrogate of fetal exposure) was increased only ~2-fold [52]. Chapy et al. reported that the knockout of *Abcb1a/1b* increased [³H]-verapamil distribution across the BBB and blood-retinal barrier (BRB) ~10- and ~1.5-fold, respectively [34]. Thus, our results regarding dissimilar impacts of P-gp on NBUP distribution across the BBB and BPB are consistent with previous studies. It appears that the BBB is generally tighter than other tissue barriers such as BPB and BRB.

The dissimilar impacts of P-gp on drug distribution across different tissue barriers may be explained by the following factors. First, this differential effect could be attributable to differences in P-gp protein expression. To test this possibility, we performed absolute protein quantification of P-gp (both *Abcb1a* and *Abcb1b*) in maternal mouse brain and placenta tissues by LC-MS/MS proteomics. After having taken into account of the percentage of trophoblasts or brain microvessels out of total cells in mouse placenta or maternal brain, respectively, we found that the density of *Abcb1a/1b* protein in the BPB was ~6.3 times lower than that in the BBB (Fig. 5b), contributing at least in part to the difference in impact of P-gp on NBUP exposure between the fetus and maternal brain. However, this difference in P-gp density is possibly an overestimation, as not all trophoblasts in the labyrinth zone of mouse placenta form the BPB. Second, physical characteristics of tissue barriers could also have an effect. It is a general consensus that the BBB possesses the tightest junction between brain capillary endothelial cells. In contrast, the BPB possesses numerous paracellular junctions which are quite different from the brain endothelial junctions, showing no positional preference (luminal or abluminal) and being interspersed with adherens junctions along the paracellular cleft [53]. These clefts would allow significant passive diffusion of drug molecules across the BPB. Hence, the fraction of drug transported by P-gp across the

BPB may be smaller than that across the BBB, resulting in smaller effects of P-gp on drug distribution across the BPB versus the BBB. Finally, other factors such as tissue blood flow rate and expression of other transporters may also play a role. The placenta is a much more perfused organ than the brain, and hence placenta blood flow rate would be expected to facilitate passive diffusion, thus decreasing the impact of transporters. If the knockout of *Abcb1a/1b* alters expression of other efflux or uptake transporters in the BBB and BPB that are able to transport NBUP, this could also affect the role of P-gp in determining fetal or brain exposure. We would like to point out that whether P-gp exerts dissimilar impacts on brain and fetal drug exposure could possibly be drug-dependent. Previous studies have shown that the knockout of P-gp increased fetal concentrations of paclitaxel at a single time point ~16-fold [17] and brain exposure (AUC) ~8-fold [54]. Thus, P-gp could have a comparable or a greater effect on fetal exposure to paclitaxel compared to brain exposure to paclitaxel. Nevertheless, since the previous study only analyzed paclitaxel fetal concentrations at single time points [17], definitive comparisons between NBUP and paclitaxel could not be made. Overall, a great degree of caution should be taken in interpretation of dissimilar impacts of P-gp in different tissue barriers.

Fetal NBUP-G exposure was ~54 times higher than fetal NBUP exposure in the wild-type mice, and this was not affected by the knockout of *Abcb1a/1b* or *Abcb1a/1b/Abcg2* (Table 5). Given that maternal plasma exposure of NBUP-G was only 5-9 times higher than maternal plasma exposure of NBUP in wild-type and *Abcb1a^{-/-}/1b^{-/-}* or *Abcb1a^{-/-}/1b^{-/-}/Abcg2^{-/-}* mice (Table 2), this drastic increase in fetal NBUP-G exposure cannot be explained solely by the increase in maternal NBUP-G exposure. Since fetal NBUP exposure was actually decreased in pregnant mice of all three genotypes compared to maternal NBUP exposure (with a fetal-to-maternal plasma AUC ratio of 0.5-0.6) (Table 5), the drastic increase in fetal NBUP-G exposure is likely caused by metabolism of NBUP in the fetus and/or placenta, rather than maternal plasma driven. Buckley et al. [55] have shown that Ugt1a, Ugt2a, Ugt2b and Ugt3a are expressed in mouse placenta. Although studies of rodent fetal livers showed glucuronidation activity, expression of specific Ugt isoforms in mouse fetal livers has not yet been fully described [56, 57]. In *Abcb1a^{-/-}/1b^{-/-}* and *Abcb1a^{-/-}/1b^{-/-}/Abcg2^{-/-}* mice, maternal plasma AUC of NBUP-G was increased 3-4-fold compared to wild-type mice (Table 2); however, fetal AUC of NBUP-G was increased only 1.7-2.0-fold (Table 5), indicating a low membrane permeability of NBUP-G which makes sense as NBUP-G is much more water soluble than its parent NBUP. Unlike in the brain, the additional knockout of *Abcg2* only slightly increased fetal NBUP-G exposure, suggesting that BCRP is not a major determinant for fetal NBUP-G exposure. These results suggest that NBUP metabolism in the fetus and/or placenta could play a significant role in determining fetal exposure to NBUP-G.

4. Conclusion

In the present study, we have shown that fetal exposure to NBUP and NBUP-G in pregnant mice accounts for ~60% and ~700% of maternal plasma exposure, respectively, suggesting that fetal exposure to the two major active metabolites of BUP is substantial and hence caution should be taken regarding fetal safety of the use of BUP during pregnancy. We have also demonstrated significant differential impacts of P-gp on fetal and brain exposure to

NBUP, with a much greater role of P-gp in restricting NBUP distribution across the BBB versus the BPB. This dissimilar effect may be attributable, in part, to the difference in P-gp protein expression in the tissue barriers, with a greater density of P-gp in the BBB than in the BPB. NBUP metabolism in the fetus and/or placenta likely plays a very important role in determining fetal exposure to its metabolite NBUP-G. Results of this study suggest that co-administration of selective inhibitors or inducers of P-gp may result in enhanced or decreased brain penetration of NBUP, respectively, thus affecting maternal tolerance to the opiate that is actively transported by P-gp. Such modulation of P-gp expression or activity may be significantly less effective in changing fetal exposure to this opiate.

Acknowledgments

This work was supported by the National Institutes of Health [grant number DA032507] and the National Center for Advancing Translational Sciences of the National Institutes of Health [TL1TR000422]. We gratefully thank Dr. Jashvant D. Unadkat and the University Of Washington Pharmacokinetics Of Drugs Of Abuse during Pregnancy program (UWPKDAP) for the scientific discussions.

References

1. Minozzi S, Amato L, Bellisario C, Ferri M, Davoli M. Maintenance agonist treatments for opiate-dependent pregnant women. *Cochrane Database Syst Rev*. 2013;CD006318. [PubMed: 24366859]
2. Chiang CN, Hawks RL. Pharmacokinetics of the combination tablet of buprenorphine and naloxone. *Drug Alcohol Depend*. 2003; 70:S39–47. [PubMed: 12738349]
3. Aubin HJ, Karila L, Reynaud M. Pharmacotherapy for smoking cessation: present and future. *Curr Pharm Des*. 2011; 17:1343–1350. [PubMed: 21524268]
4. Jones HE, Finnegan LP, Kaltenbach K. Methadone and buprenorphine for the management of opioid dependence in pregnancy. *Drugs*. 2012; 72:747–757. [PubMed: 22512363]
5. Cowan A. Buprenorphine: the basic pharmacology revisited. *J Addict Med*. 2007; 1:68–72. [PubMed: 21768937]
6. Brown SM, Campbell SD, Crafford A, Regina KJ, Holtzman MJ, Kharasch ED. P-glycoprotein is a major determinant of norbuprenorphine brain exposure and antinociception. *J Pharmacol Exp Ther*. 2012; 343:53–61. [PubMed: 22739506]
7. Yassen A, Kan J, Olofsen E, Suidgeest E, Dahan A, Danhof M. Pharmacokinetic-pharmacodynamic modeling of the respiratory depressant effect of norbuprenorphine in rats. *J Pharmacol Exp Ther*. 2007; 321:598–607. [PubMed: 17283225]
8. Ohtani M, Kotaki H, Nishitateno K, Sawada Y, Iga T. Kinetics of Respiratory Depression in Rats Induced by Buprenorphine and its Metabolite, Norbuprenorphine. *Journal of Pharmacology and Experimental Therapeutics*. 1997; 281:428–433. [PubMed: 9103526]
9. Kim HK, Smiddy M, Hoffman RS, Nelson LS. Buprenorphine may not be as safe as you think: a pediatric fatality from unintentional exposure. *Pediatrics*. 2012; 130:e1700–1703. [PubMed: 23129079]
10. Concheiro M, Jones H, Johnson RE, Shakleya DM, Huestis MA. Confirmatory analysis of buprenorphine, norbuprenorphine, and glucuronide metabolites in plasma by LCMSMS. Application to umbilical cord plasma from buprenorphine-maintained pregnant women. *J Chromatogr B Analyt Technol Biomed Life Sci*. 2010; 878:13–20.
11. Mao Q, Unadkat JD. Role of the breast cancer resistance protein (ABCG2) in drug transport. *Aaps j*. 2005; 7:E118–133. [PubMed: 16146333]
12. Li XQ, Wang L, Lei Y, Hu T, Zhang FL, Cho CH, To KK. Reversal of P-gp and BCRP-mediated MDR by tariquidar derivatives. *Eur J Med Chem*. 2015; 101:560–572. [PubMed: 26197160]
13. Membrane transporters in drug development. *Nat Rev Drug Discov*. 2010; 9:215–236. [PubMed: 20190787]

14. Maliapaard M, Scheffer GL, Faneyte IF, van Gastelen MA, Pijnenborg AC, Schinkel AH, van De Vijver MJ, Scheper RJ, Schellens JH. Subcellular localization and distribution of the breast cancer resistance protein transporter in normal human tissues. *Cancer Res.* 2001; 61:3458–3464. [PubMed: 11309308]
15. Cascorbi I. P-glycoprotein: tissue distribution, substrates, and functional consequences of genetic variations. *Handb Exp Pharmacol.* 2011:261–283. [PubMed: 21103972]
16. Mao Q. BCRP/ABCG2 in the placenta: expression, function and regulation. *Pharm Res.* 2008; 25:1244–1255. [PubMed: 18202831]
17. Smit JW, Huisman MT, van Tellingen O, Wiltshire HR, Schinkel AH. Absence or pharmacological blocking of placental P-glycoprotein profoundly increases fetal drug exposure. *J Clin Invest.* 1999; 104:1441–1447. [PubMed: 10562306]
18. Zhou L, Narahariseti SB, Wang H, Unadkat JD, Hebert MF, Mao Q. The breast cancer resistance protein (Bcrp1/Abcg2) limits fetal distribution of glyburide in the pregnant mouse: an Obstetric-Fetal Pharmacology Research Unit Network and University of Washington Specialized Center of Research Study. *Mol Pharmacol.* 2008; 73:949–959. [PubMed: 18079276]
19. Zhang Y, Wang H, Unadkat JD, Mao Q. Breast cancer resistance protein 1 limits fetal distribution of nitrofurantoin in the pregnant mouse. *Drug Metab Dispos.* 2007; 35:2154–2158. [PubMed: 17785426]
20. Agarwal S, Sane R, Ohlfest JR, Elmquist WF. The role of the breast cancer resistance protein (ABCG2) in the distribution of sorafenib to the brain. *J Pharmacol Exp Ther.* 2011; 336:223–233. [PubMed: 20952483]
21. Kodaira H, Kusuhara H, Ushiki J, Fuse E, Sugiyama Y. Kinetic analysis of the cooperation of P-glycoprotein (P-gp/Abcb1) and breast cancer resistance protein (Bcrp/Abcg2) in limiting the brain and testis penetration of erlotinib, flavopiridol, and mitoxantrone. *J Pharmacol Exp Ther.* 2010; 333:788–796. [PubMed: 20304939]
22. Tourmier N, Chevillard L, Megarbane B, Pirnay S, Scherrmann JM, Declèves X. Interaction of drugs of abuse and maintenance treatments with human P-glycoprotein (ABCB1) and breast cancer resistance protein (ABCG2). *Int J Neuropsychopharmacol.* 2010; 13:905–915. [PubMed: 19887017]
23. Mao Q, Unadkat JD. Role of the Breast Cancer Resistance Protein (BCRP/ABCG2) in Drug Transport—an Update. *The AAPS Journal.* 2015; 17:65–82. [PubMed: 25236865]
24. Nakanishi H, Yonezawa A, Matsubara K, Yano I. Impact of P-glycoprotein and breast cancer resistance protein on the brain distribution of antiepileptic drugs in knockout mouse models. *Eur J Pharmacol.* 2013; 710:20–28. [PubMed: 23588114]
25. Zhou L, Schmidt K, Nelson FR, Zelesky V, Troutman MD, Feng B. The Effect of Breast Cancer Resistance Protein and P-Glycoprotein on the Brain Penetration of Flavopiridol, Imatinib Mesylate (Gleevec), Prazosin, and 2-Methoxy-3-(4-(2-(5-methyl-2-phenyloxazol-4-yl)ethoxy)phenyl)propanoic Acid (PF-407288) in Mice. *Drug Metabolism and Disposition.* 2009; 37:946–955. [PubMed: 19225039]
26. Schinkel AH, Smit JJ, van Tellingen O, Beijnen JH, Wagenaar E, van Deemter L, Mol CA, van der Valk MA, Robanus-Maandag EC, te Riele HP, et al. Disruption of the mouse mdr1a P-glycoprotein gene leads to a deficiency in the blood-brain barrier and to increased sensitivity to drugs. *Cell.* 1994; 77:491–502. [PubMed: 7910522]
27. Kort A, Sparidans RW, Wagenaar E, Beijnen JH, Schinkel AH. Brain accumulation of the EML4-ALK inhibitor ceritinib is restricted by P-glycoprotein (P-GP/ABCB1) and breast cancer resistance protein (BCRP/ABCG2). *Pharmacol Res.* 2015; 102:200–207. [PubMed: 26361725]
28. Thompson SJ, Koszdin K, Bernards CM. Opiate-induced analgesia is increased and prolonged in mice lacking P-glycoprotein. *Anesthesiology.* 2000; 92:1392–1399. [PubMed: 10781286]
29. Rodriguez M, Ortega I, Soengas I, Suarez E, Lukas JC, Calvo R. Effect of P-glycoprotein inhibition on methadone analgesia and brain distribution in the rat. *J Pharm Pharmacol.* 2004; 56:367–374. [PubMed: 15025862]
30. Schinkel AH, Wagenaar E, van Deemter L, Mol CA, Borst P. Absence of the mdr1a P-Glycoprotein in mice affects tissue distribution and pharmacokinetics of dexamethasone, digoxin, and cyclosporin A. *J Clin Invest.* 1995; 96:1698–1705. [PubMed: 7560060]

31. Dagenais C, Graff CL, Pollack GM. Variable modulation of opioid brain uptake by P-glycoprotein in mice. *Biochem Pharmacol.* 2004; 67:269–276. [PubMed: 14698039]
32. Hamabe W, Maeda T, Fukazawa Y, Kumamoto K, Shang LQ, Yamamoto A, Yamamoto C, Tokuyama S, Kishioka S. P-glycoprotein ATPase activating effect of opioid analgesics and their P-glycoprotein-dependent antinociception in mice. *Pharmacol Biochem Behav.* 2006; 85:629–636. [PubMed: 17134744]
33. Kharasch ED, Hoffer C, Altuntas TG, Whittington D. Quinidine as a probe for the role of p-glycoprotein in the intestinal absorption and clinical effects of fentanyl. *J Clin Pharmacol.* 2004; 44:224–233. [PubMed: 14973303]
34. Chapy H, Saubamea B, Tournier N, Bourasset F, Behar-Cohen F, Decleves X, Scherrmann JM, Cisternino S. Blood-brain and retinal barriers show dissimilar ABC transporter impacts and concealed effect of P-glycoprotein on a novel verapamil influx carrier. *Br J Pharmacol.* 2016; 173:497–510. [PubMed: 26507673]
35. Kalabis GM, Kostaki A, Andrews MH, Petropoulos S, Gibb W, Matthews SG. Multidrug Resistance Phosphoglycoprotein (ABCB1) in the Mouse Placenta: Fetal Protection. *Biology of Reproduction.* 2005; 73:591–597. [PubMed: 15917342]
36. Zhang H, Wu X, Wang H, Mikheev AM, Mao Q, Unadkat JD. Effect of pregnancy on cytochrome P450 3a and P-glycoprotein expression and activity in the mouse: mechanisms, tissue specificity, and time course. *Molecular pharmacology.* 2008; 74:714–723. [PubMed: 18509067]
37. Wang H, Wu X, Hudkins K, Mikheev A, Zhang H, Gupta A, Unadkat JD, Mao Q. Expression of the breast cancer resistance protein (Bcrp1/Abcg2) in tissues from pregnant mice: effects of pregnancy and correlations with nuclear receptors. *Am J Physiol Endocrinol Metab.* 2006; 291:E1295–1304. [PubMed: 17082346]
38. Alhaddad H, Cisternino S, Decleves X, Tournier N, Schlatter J, Chiadmi F, Risede P, Smirnova M, Besengez C, Scherrmann JM, et al. Respiratory toxicity of buprenorphine results from the blockage of P-glycoprotein-mediated efflux of norbuprenorphine at the blood-brain barrier in mice. *Crit Care Med.* 2012; 40:3215–3223. [PubMed: 22975888]
39. Concheiro M, Jones HE, Johnson RE, Choo R, Huestis MA. Preliminary buprenorphine sublingual tablet pharmacokinetic data in plasma, oral fluid and sweat during treatment of opioid-dependent pregnant women. *Therapeutic drug monitoring.* 2011; 33:619–626. [PubMed: 21860340]
40. Ohtani M, Kotaki H, Uchino K, Sawada Y, Iga T. Pharmacokinetic analysis of enterohepatic circulation of buprenorphine and its active metabolite, norbuprenorphine, in rats. *Drug Metab Dispos.* 1994; 22:2–7. [PubMed: 8149883]
41. Brown SM, Holtzman M, Kim T, Kharasch ED. Buprenorphine metabolites, buprenorphine-3-glucuronide and norbuprenorphine-3-glucuronide, are biologically active. *Anesthesiology.* 2011; 115:1251–1260. [PubMed: 22037640]
42. Prasad B, Evers R, Gupta A, Hop CECA, Salphati L, Shukla S, Ambudkar SV, Unadkat JD. Interindividual Variability in Hepatic Organic Anion-Transporting Polypeptides and P-Glycoprotein (ABCB1) Protein Expression: Quantification by Liquid Chromatography Tandem Mass Spectroscopy and Influence of Genotype, Age, and Sex. *Drug Metabolism and Disposition.* 2014; 42:78–88. [PubMed: 24122874]
43. Wang L, Prasad B, Salphati L, Chu X, Gupta A, Hop CE, Evers R, Unadkat JD. Interspecies variability in expression of hepatobiliary transporters across human, dog, monkey, and rat as determined by quantitative proteomics. *Drug Metab Dispos.* 2015; 43:367–374. [PubMed: 25534768]
44. Shuster DL, Rislis LJ, Liang CK, Rice KM, Shen DD, Hebert MF, Thummel KE, Mao Q. Maternal-fetal disposition of glyburide in pregnant mice is dependent on gestational age. *J Pharmacol Exp Ther.* 2014; 350:425–434. [PubMed: 24898265]
45. Iguchi T, Tani N, Sato T, Fukatsu N, Ohta Y. Developmental changes in mouse placental cells from several stages of pregnancy in vivo and in vitro. *Biology of Reproduction.* 1993; 48:188–196. [PubMed: 8418907]
46. Goffinet, AM., Rakic, P. *Mouse Brain Development.* Springer; Berlin, Heidelberg: 2000.

47. Cordon-Cardo C, O'Brien JP, Casals D, Rittman-Grauer L, Biedler JL, Melamed MR, Bertino JR. Multidrug-resistance gene (P-glycoprotein) is expressed by endothelial cells at blood-brain barrier sites. *Proc Natl Acad Sci U S A*. 1989; 86:695–698. [PubMed: 2563168]
48. Novotna M, Libra A, Kopecky M, Pavek P, Fendrich Z, Semecky V, Staud F. P-glycoprotein expression and distribution in the rat placenta during pregnancy. *Reprod Toxicol*. 2004; 18:785–792. [PubMed: 15279876]
49. Jones HE, Kaltenbach K, Heil SH, Stine SM, Coyle MG, Arria AM, O'Grady KE, Selby P, Martin PR, Fischer G. Neonatal Abstinence Syndrome after Methadone or Buprenorphine Exposure. *The New England journal of medicine*. 2010; 363:2320–2331. [PubMed: 21142534]
50. Jones HE, Arria AM, Baewert A, Heil SH, Kaltenbach K, Martin PR, Coyle MG, Selby P, Stine SM, Fischer G. Buprenorphine Treatment of Opioid-Dependent Pregnant Women: A Comprehensive Review. *Addiction (Abingdon, England)*. 2012; 107:5–27.
51. Concheiro M, Jones HE, Johnson RE, Choo R, Shakleya DM, Huestis MA. Maternal Buprenorphine Dose, Placenta Buprenorphine and Metabolite Concentrations and Neonatal Outcomes. *Therapeutic drug monitoring*. 2010; 32:206–215. [PubMed: 20216119]
52. Eyal S, Chung FS, Muzi M, Link JM, Mankoff DA, Kaddoumi A, O'Sullivan F, Hebert MF, Unadkat JD. Simultaneous PET Imaging of P-Glycoprotein Inhibition in Multiple Tissues in the Pregnant Non-Human Primate. *Journal of nuclear medicine : official publication, Society of Nuclear Medicine*. 2009; 50:798–806.
53. Leach L. The phenotype of the human materno-fetal endothelial barrier: molecular occupancy of paracellular junctions dictate permeability and angiogenic plasticity. *J Anat*. 2002; 200:599–606. [PubMed: 12162727]
54. Kemper EM, van Zandbergen AE, Cleypool C, Mos HA, Boogerd W, Beijnen JH, van Tellingen O. Increased penetration of paclitaxel into the brain by inhibition of P-Glycoprotein. *Clin Cancer Res*. 2003; 9:2849–2855. [PubMed: 12855665]
55. Buckley DB, Klaassen CD. Tissue- and Gender-Specific mRNA Expression of UDP-Glucuronosyltransferases (UGTs) in Mice. *Drug Metabolism and Disposition*. 2007; 35:121–127. [PubMed: 17050650]
56. Collier AC, Milam KA, Rougée LRA, Sugawara A, Yamauchi Y, Ward MA. Upregulation of Ugt1a genes in placentas and fetal livers in a murine model of assisted reproduction. *Placenta*. 2012; 33:77–80. [PubMed: 22115498]
57. Collier AC, Yamauchi Y, Sato BLM, Rougée LRA, Ward MA. UDP-Glucuronosyltransferase 1a Enzymes Are Present and Active in the Mouse Blastocyst. *Drug Metabolism and Disposition*. 2014; 42:1921–1925. [PubMed: 25200869]

Abbreviations

ABC	ATP-binding cassette
AUC	area under the concentration-time curve
BBB	the blood- brain barrier
BPB	the blood-placental barrier
P-gp	P-glycoprotein
BCRP	breast cancer resistance protein
ABCB1	the first member of subfamily B of the ABC transporter superfamily
ABCG2	the second member of subfamily G of the ABC transporter superfamily
<i>Abcb1a</i>	the murine isoform a of the human <i>ABCB1</i> gene

<i>Abcb1b</i>	the murine isoform b of the human <i>ABCB1</i> gene
PBS	phosphate-buffered saline
LC-MS	Liquid chromatography-mass spectrometry
HPLC	high-performance liquid chromatography
BUP	buprenorphine
NBUP	norbuprenorphine
NBUP-d3	norbuprenorphine-d3, NBUP-G, norbuprenorphine-3- β -D-glucuronide
gd	gestation day
DMSO	dimethyl sulfoxide
SIL	stable isotope-labeled
SPE	solid-phase extraction

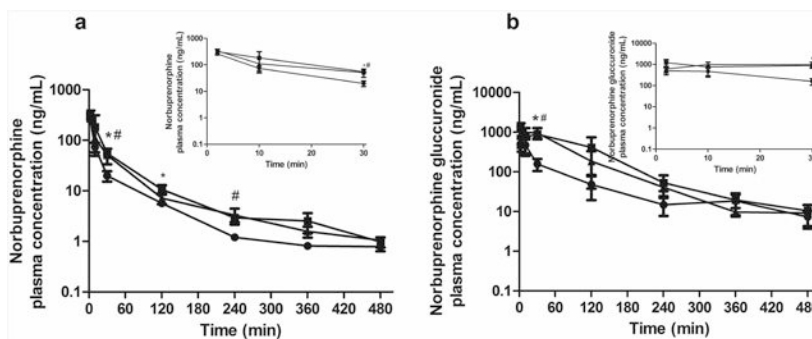


Figure 1. Maternal plasma concentration-time profiles

Shown are maternal plasma concentration-time profiles of norbuprenorphine (a) and norbuprenorphine- β -D-glucuronide (b) over 480 min after retro-orbital injection of 1 mg/kg norbuprenorphine to pregnant wild-type (circle), *Abcb1a*^{-/-}/*1b*^{-/-} (triangle) and *Abcb1a*^{-/-}/*1b*^{-/-}/*Abcg2*^{-/-} (square) mice. Data are shown as means \pm SD from three mice at each time point. Statistically significant differences between wild-type and *Abcb1a*^{-/-}/*1b*^{-/-} or *Abcb1a*^{-/-}/*1b*^{-/-}/*Abcg2*^{-/-} mice were analyzed by ANOVA analysis for multiple comparisons followed by a Bonferroni correction assuming a significance of 0.05. * indicates $p < 0.05$ for *Abcb1a*^{-/-}/*1b*^{-/-} mice; # indicates $p < 0.05$ for *Abcb1a*^{-/-}/*1b*^{-/-}/*Abcg2*^{-/-} mice. Inserts show early time points up to 30 min in an expanded format.

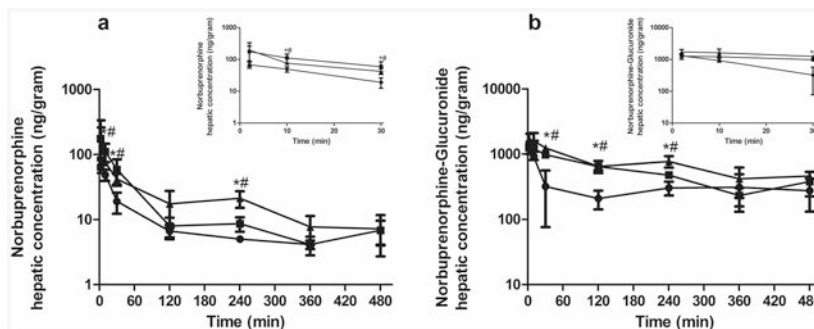


Figure 2. Maternal liver concentration-time profiles

Shown are maternal liver concentrations of norbuprenorphine (a) and norbuprenorphine- β -D-glucuronide (b) over 480 min after retro-orbital injection of 1 mg/kg norbuprenorphine to pregnant wild-type (circle), *Abcb1a*^{-/-}/*1b*^{-/-} (triangle) and *Abcb1a*^{-/-}/*1b*^{-/-}/*Abcg2*^{-/-} (square) mice. Data are shown as means \pm SD from three mice at each time point. Statistically significant differences between wild-type and *Abcb1a*^{-/-}/*1b*^{-/-} or *Abcb1a*^{-/-}/*1b*^{-/-}/*Abcg2*^{-/-} mice were analyzed by ANOVA analysis for multiple comparisons followed by a Bonferroni correction assuming a significance of 0.05. * indicates $p < 0.05$ for *Abcb1a*^{-/-}/*1b*^{-/-} mice; # indicates $p < 0.05$ for *Abcb1a*^{-/-}/*1b*^{-/-}/*Abcg2*^{-/-} mice. Inserts show early time points up to 30 min in an expanded format.

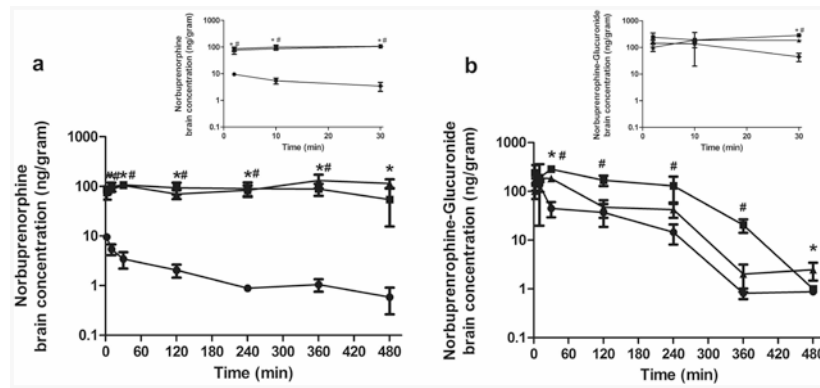


Figure 3. Maternal brain concentration-time profiles

Shown are maternal brain concentration-time profiles of norbuprenorphine (**a**) and norbuprenorphine- β -D-glucuronide (**b**) over 480 min after retro-orbital injection of 1 mg/kg norbuprenorphine pregnant wild-type (circle), *Abcb1a*^{-/-}/*1b*^{-/-} (triangle) and *Abcb1a*^{-/-}/*1b*^{-/-}/*Abcg2*^{-/-} (square) mice. Data are shown as means \pm SD from three mice at each time point. Statistically significant differences between wild-type and *Abcb1a*^{-/-}/*1b*^{-/-} or *Abcb1a*^{-/-}/*1b*^{-/-}/*Abcg2*^{-/-} mice were analyzed by ANOVA analysis for multiple comparisons followed by a Bonferroni correction assuming a significance of 0.05. * indicates $p < 0.05$ for *Abcb1a*^{-/-}/*1b*^{-/-} mice; # indicates $p < 0.05$ for *Abcb1a*^{-/-}/*1b*^{-/-}/*Abcg2*^{-/-} mice. Inserts show early time points up to 30 min in an expanded format.

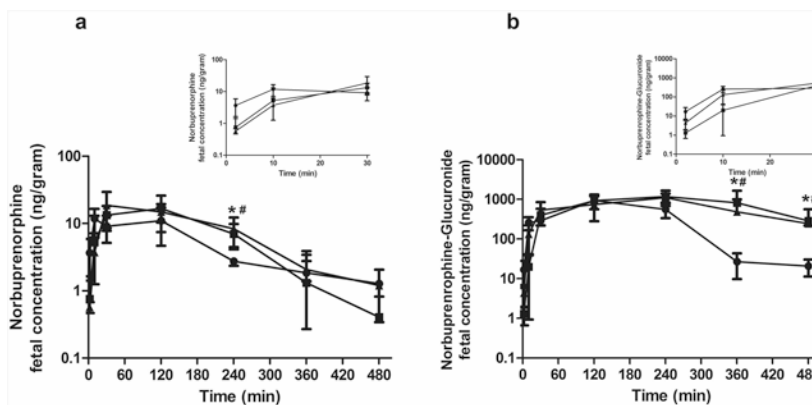


Figure 4. Fetal concentration-time profiles

Shown are fetal concentration-time profiles of norbuprenorphine (a) and norbuprenorphine- β -D-glucuronide (b) over 480 min after retro-orbital injection of 1 mg/kg norbuprenorphine to pregnant wild-type (circle), *Abcb1a*^{-/-}/*1b*^{-/-} (triangle) and *Abcb1a*^{-/-}/*1b*^{-/-}/*Abcg2*^{-/-} (square) mice. Data are shown as means \pm SD from three mice at each time point. Statistically significant differences between wild-type and *Abcb1a*^{-/-}/*1b*^{-/-} or *Abcb1a*^{-/-}/*1b*^{-/-}/*Abcg2*^{-/-} mice were analyzed by ANOVA analysis for multiple comparisons followed by a Bonferroni correction assuming a significance of 0.05. * indicates $p < 0.05$ for *Abcb1a*^{-/-}/*1b*^{-/-} mice; # indicates $p < 0.05$ for *Abcb1a*^{-/-}/*1b*^{-/-}/*Abcg2*^{-/-} mice. Inserts show early time points up to 30 min in an expanded format.

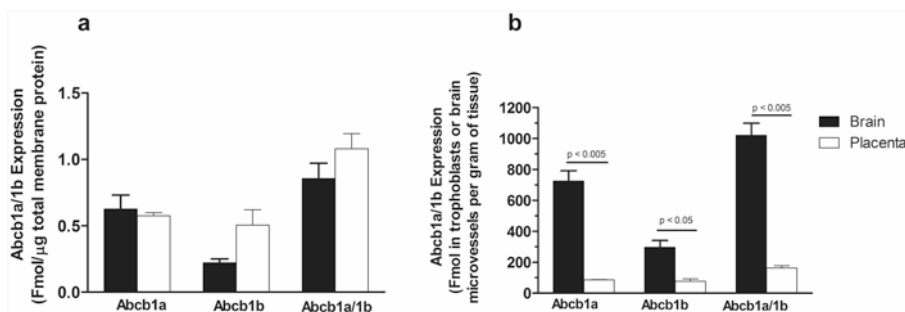


Figure 5. Absolute protein quantification of Abcb1a and Abcb1b protein in maternal brain and placenta

Shown are absolute protein quantifications of Abcb1a and Abcb1b in maternal brain (black bar) and placenta (open bar) in total membrane proteins (a) or estimated abundance of Abcb1a and/or Abcb1b in cells that form the mouse blood-brain and blood-placental barriers (b). Data shown are means \pm SD in tissues collected from four different mice. Statistically significant differences between maternal brain and placenta were analyzed by unpaired Student *t*-test. Differences with *p* values of < 0.05 were considered statistically significant.

Table 1
Surrogate peptides of Abc1a and Abc1b and their MS/MS parameters

Protein name	Surrogate peptide	Peptide type	Parent ion (<i>m/z</i>)	Fragment ion (<i>m/z</i>)	Declustering potential (V)	Collision energy (V)
Abc1a	NTTGLTTR	Light	467.75	719.41	60	21
Abc1a	NTTGLTTR	Light	467.75	618.36	60	21
Abc1a	NTTGLTTR	Light	467.75	490.3	60	21
Abc1a	NTTGLTTR	Heavy	472.75	729.42	60	21
Abc1a	NTTGLTTR	Heavy	472.75	628.37	60	21
Abc1b	NSTGSLTTR	Light	468.74	634.35	60	21
Abc1b	NSTGSLTTR	Light	468.74	735.4	60	21
Abc1b	NSTGSLTTR	Light	468.74	577.33	60	21
Abc11b	NSTGSLTTR	Heavy	473.74	644.36	60	21
Abc1b	NSTGSLTTR	Heavy	473.74	745.41	60	21

Maternal plasma AUCs of norbuprenorphine (NBUP) and norbuprenorphine-3- β -D-glucuronide (NBUP-G) after retro-orbital injection (1 mg/kg) to pregnant mice on gd 15 over 480 min. Data are reported as mean (95% confidence interval). The NBUP-G/NBUP AUC ratios were calculated based on molar concentrations of NBUP and NBUP-G in maternal plasma. Differences between the analyte AUCs or the AUC ratios of wild-type and *Abcb1a*^{-/-}/*Ib*^{-/-} or *Abcb1a*^{-/-}/*Ib*^{-/-}/*Abcg2*^{-/-} mice were calculated using bootstrapping as described in the Materials and methods section. The *p* values were corrected for multiple testing using the Bonferroni method.

Table 2

Parameter	Genotype		
	Wild-type	<i>Abcb1a</i> ^{-/-} / <i>Ib</i> ^{-/-}	<i>Abcb1a</i> ^{-/-} / <i>Ib</i> ^{-/-} / <i>Abcg2</i> ^{-/-}
AUC0-480min of NBUP ($\mu\text{g}\times\text{min}\times\text{mL}^{-1}$)	4.1 [3.6, 5.8]	7.1 [6.2, 9.4]	8.7 [7.1, 11.3]
Fold-change	1.0	1.8	2.2
AUC0-480min of NBUP-G ($\mu\text{g}\times\text{min}\times\text{mL}^{-1}$)	26.8 [21.8, 34.2]	95.0 [75.5, 120.8]	116.7 [84.4, 154.1]
Fold-change	1.0	3.6	4.4
NBUP-G/NBUP maternal plasma AUC ratio	4.6 [3.7, 5.8]	9.4 [7.1, 11.3]	9.4 [6.1, 13.5]
Fold-change	1.0	2.0	2.0
		<i>p</i>	<i>p</i>
		< 0.005	< 0.005
		< 0.0001	< 0.0001
		0.09	0.3

Table 3

Maternal liver tissue AUCs of norbuprenorphine (NBUP) and norbuprenorphine-3- β -D-glucuronide (NBUP-G) after retro-orbital injection (1 mg/kg) to pregnant mice on gd 15 over 480 min. Data are reported as mean (95% confidence interval). Differences between the analyte AUCs or the AUC ratios of wild-type and *Abcb1a*^{-/-}/*Ib*^{-/-} or *Abcb1a*^{-/-}/*Ib*^{-/-}/*Abcg2*^{-/-} mice were calculated using bootstrapping as described in the Materials and methods section. The *p* values were corrected for multiple testing using the Bonferroni method.

Parameter	Genotype		
	Wild-type	<i>Abcb1a</i> ^{-/-} / <i>Ib</i> ^{-/-}	<i>Abcb1a</i> ^{-/-} / <i>Ib</i> ^{-/-} / <i>Abcg2</i> ^{-/-}
AUC0-480min of NBUP ($\mu\text{g}\times\text{min}\times\text{g}^{-1}$)	4.2 [3.6, 5.1]	9.9 [8.4, 11.8]	8.3 [6.7, 10.2]
Fold-change	1.0	2.3	2.0
AUC0-480min of NBUP-G ($\mu\text{g}\times\text{min}\times\text{g}^{-1}$)	148.4 [118.9, 179.2]	338.0 [297.2, 376.8]	252.4 [229.4, 272.8]
Fold-change	1.0	2.3	1.7
			<i>p</i>
			< 0.005
			< 0.0001

Maternal brain AUCs of norbuprenorphine (NBUP) and norbuprenorphine-3- β -D-glucuronide (NBUP-G) after retro-orbital injection (1 mg/kg) to pregnant mice on gd 15 over 480 min. Data are reported as mean (95% confidence interval). Differences between the analyte AUCs or the AUC ratios of wild-type and *Abcb1a^{-/-}/Ib^{-/-}* or *Abcb1a^{-/-}/Ib^{-/-}/Abcg2^{-/-}* mice were calculated using bootstrapping as described in the Materials and methods section. The *p* values were corrected for multiple testing using the Bonferroni method.

Table 4

Parameter	Genotype		
	Wild-type	<i>Abcb1a^{-/-}/Ib^{-/-}</i>	<i>Abcb1a^{-/-}/Ib^{-/-}/Abcg2^{-/-}</i>
Brain AUC _{0-480min} of NBUP ($\mu\text{g}\times\text{min}\times\text{g}^{-1}$)	0.8 [0.7, 0.9]	47.3 [39.9, 52.4]	42.8 [37.0, 47.9]
Fold-change	1.0	60.1	54.4
Brain/Maternal plasma AUC ratio of NBUP	0.2 [0.1, 0.3]	6.7 [4.7, 8.1]	4.9 [3.2, 6.5]
Fold-change	1.0	34.1	24.5
Brain AUC _{0-480min} of NBUP-G ($\mu\text{g}\times\text{min}\times\text{g}^{-1}$)	10.7 [8.4, 13.1]	23.6 [20.6, 27.4]	56.1 [48.1, 66.3]
Fold-change	1.0	2.2	5.2
Brain/Maternal plasma AUC ratio of NBUP-G	0.4 [0.3, 0.5]	0.25 [0.18, 0.37]	0.26 [0.36, 0.65]
Fold-change	1.0	0.6	1.2
			<i>p</i>
			< 0.0001
			< 0.01
			< 0.005
			0.9

Fetal AUCs of norbuprenorphine (NBUP) and norbuprenorphine-3- β -D-glucuronide (NBUP-G) after retro-orbital injection (1 mg/kg) to pregnant mice on gd 15 over 480 min. Data are reported as mean (95% confidence interval). The NBUP-G/NBUP AUC ratios were calculated based on molar concentrations of NBUP and NBUP-G in the fetus. Differences between the analyte AUCs or the AUC ratios of wild-type and *Abcb1a*^{-/-}/*Ib*^{-/-} or *Abcb1a*^{-/-}/*Ib*^{-/-}/*Abcg2*^{-/-} mice were calculated using bootstrapping as described in the Materials and methods section. The *p* values were corrected for multiple testing using the Bonferroni method.

Table 5

Parameter	Genotype			
	Wild-type	<i>Abcb1a</i> / <i>Ib</i> ^{-/-}	<i>Abcb1a</i> / <i>Ib</i> ; <i>Abcg2</i> ^{-/-}	<i>p</i>
Fetal AUC0-480min of NBUP ($\mu\text{g}\times\text{min}\times\text{g}^{-1}$)	2.5 [2.0, 2.9]	4.0 [3.5, 4.5]	4.1 [3.5, 4.6]	<0.005
Fold-change	1.0	1.6	1.6	
Fetal/Maternal plasma AUC ratio of NBUP	0.64 [0.40, 0.83]	0.56 [0.39, 0.63]	0.45 [0.28, 0.60]	0.6
Fold-change	1.0	0.87	0.71	
Fetal AUC0-480min of NBUP-G ($\mu\text{g}\times\text{min}\times\text{g}^{-1}$)	189.2 [159.2, 199.2]	314.5 [266.0, 363.1]	373.5 [287.6, 485.1]	<0.0001
Fold-change	1.0	1.7	2.0	
Fetal/Maternal plasma AUC ratio of NBUP-G	7.2 [4.8, 9.2]	3.31 [2.1, 4.6]	3.2 [2.0, 4.8]	0.2
Fold-change	1.0	0.46	0.45	
NBUP-G/NBUP fetal AUC ratio	53.9 [53.9, 54.6]	55.9 [46.4, 66.3]	64.6 [50.2, 83.3]	0.9
Fold-change	1.0	1	1.2	